

RESEARCH ARTICLE

A Multiple Power Level Random Access Method for M2M Communications in LTE-A Network

Z. Alavikia and A. Ghasemi*

Faculties of Electrical and Computer Engineering, K.N. Toosi University of Technology, Tehran, Iran

ABSTRACT

Access Control is an effective way to protect the radio access part of Long-Term Evolution-Advanced (LTE-A) network from the overload caused by a huge number of Machine Type Communication Devices (MTC). A class of access control mechanisms is the Access Class Barring (ACB), which regulates the machine-to-machine (M2M) traffic in accordance with the available random access (RA) resources. In this paper, we extend the single power level ACB scheme to a multiple power level method in order to increase the number of successfully transmitted requests in the case of overload. Our analysis is based on the capture effect in the third step of RA procedure of the LTE-A system in which one of the transmitted requests by two or more co-tagged MTCs, MTCs which use the same preamble in the first step, can be decoded by the eNB. We first formulate the power level selection as an optimization problem assuming the perfect capture model without considering MTCs' energy budget. Then, to take into account MTCs' energy consumption, the scenario is extended for the Signal to Interference Ratio (SIR) based capture model. In addition, we investigate the advantages of the proposed multiple power level RA method on discriminating the access of MTCs with different priorities. The numerical results show that using the optimal parameters, the RA throughput can be improved in comparison with the single power level system at the cost of slightly increasing MTCs' energy consumption and the complexity of RA procedure. Copyright © 2012 John Wiley & Sons, Ltd.

*Correspondence

Faculty of Computer Engineering, K.N. Toosi University of Technology, Tehran, Iran

1. INTRODUCTION

Machine-to-Machine (M2M) communications enable the connectivity between billions of Machine-Type Communication Devices (MTC) in the context of the Internet of Things (IoT). In the IoT paradigm, MTCs will be able to measure, analysis and deliver information in an autonomous manner with minimal human interaction. M2M solutions for remote monitoring show great market opportunities in many fields such as smart metering, health care, transportation, and industrial automation [1]. In order to achieve a ubiquitous connectivity of MTCs, Long-Term Evolution (LTE) and LTE-Advanced (LTE-A) networks are envisaged to provide cost-effective solutions for the deployment of M2M applications [2].

In the LTE / LTE-A networks, unconnected MTCs may get connected to the evolved-Node B (eNB) through the Random Access (RA) procedure. In the contention-based RA procedure, the Physical Random Access Channel (PRACH) is used to transmit orthogonal preamble codes. If two or more MTCs select the same preamble code on the same PRACH opportunity simultaneously, they will grant and transmit their requests on the same

Resource Blocks (RB) of Physical Uplink Shared Channel (PUSCH). In this case, it is probable that the eNB could not detect the transmitted requests and hence the contending MTCs could not successfully pass the RA procedure [3]. Due to the slotted ALOHA-based RA contention, the performance of RA is suffering from the collisions caused by a lot of connection requests of MTCs which typically is greater than user equipments by orders of magnitude.

Collision in the RA procedure will waste the system resources, decreases MTC's energy, and increases the access delay. In order to control the RACH overload in the LTE/LTE-A caused by M2M communications, several proposals have been discussed in Third-Generation Partnership Project (3GPP) and different literature [4, 5, 6, 7]. Although, these overload control solutions mainly focus on barring requests of MTCs or increasing the number of contention resources upon overload detection to enhance the performance of RA procedure. Providing more RA resources leads to rising the costs of resource usage; while barring more MTCs increases the access delay.

In order to decrease the average access delay of MTCs without increasing the number of contention resources,

in this paper, the advantage of the power capture effect is used to improve the success probability of MTCDs in the RA procedure. According to this effect, the transmitted request of one MTCD with a high enough transmission power will be detected by the eNB, while, it has collided with other MTCDs' requests [8]. In order to benefit from the power capture effect, the number of contending MTCDs at each power level must be determined in accordance with the available RA resources. To do this, we formulate an optimization problem to find the optimum values of the ACB parameters and the corresponding selection probabilities for each power level. It is well known that the energy consumption of MTCDs is of paramount importance and depends on the specified application requirements [2, 9]. By considering the energy consumption of battery-powered MTCDs, we aim to determine the transmission power at each power level in the signal to interference (SIR) based capture model. Beside the RA throughput enhancement, we also show that the power capture effect can be used to discriminate the access of MTCDs with different priorities which is important for emergency alarm notifications as a significant application of M2M communications. It is notable to mention that in the multiple power level RA method, the eNB computes and broadcasts the power levels and their corresponding probabilities in the RA procedure which may incur additional complexity in comparison with the single power level RA procedure. The main contributions of this paper include:

- We extend the single power level ACB scheme to a multiple power level scheme to enhance the throughput of RA procedure. We first compute the optimum transmission probability for each power level assuming a simple capture model in which the interference of lower power MTCDs does not affect the successful transmission of a higher power level transmission.
- Adopting a more realistic SIR-based capture model, we then take into account the interference of the lower power MTCDs and find the transmission power and the corresponding transmission probability for each level. We show that using the proposed scheme, the average access delay and the RA throughput are enhanced compared to the single power level ACB scheme.
- Finally, we use the multiple power level RA method for the emergency applications which require higher priority in channel access against the low priority applications.

The outline of the paper is as follow. In Section 2, the related works are reviewed. The system model is presented in Section 3. Section 4 is dedicated to the proposed RA method for the perfect capture model and the SIR-based capture model. Also, in this section, the priority point of view of the proposed RA method has been investigated. The performance of the proposed method is demonstrated

in Section 5. Finally, conclusions are presented in Section 6.

2. RELATED WORKS

The deployment of a huge number of MTCDs in the LTE leads to the overload problem. There are various solutions for the overload control problem in literature, some of them have been summarized in [10]. The proposed solutions can be classified into two main categories: in the first, excessive access requests of MTCDs are barred and in the second, the number of contention resources in an overload condition is increased.

In the first category, 3GPP introduced some specific solutions to protect the radio access network of the LTE. In these solutions, the access of delay-tolerant MTCDs are barred upon overload detection. One suggestion by 3GPP working groups for the RACH overload is the ACB scheme [4]. In the ACB, the eNB broadcasts the barring probability and the barring timer to guide the MTCDs how to initiate the RA procedure. When an unconnected MTCD attempts to connect to the eNB, it uniformly selects a random number between 0 and 1. If the selected number is below the barring probability, it can initiate the RA procedure. Otherwise, it postpones its attempt for a random time. The barring timer determines the mean duration of access control. In the optimal dynamic ACB scheme, the eNB knows the number of active MTCDs in each RA procedure and hence can compute the optimum ACB barring factor taking into account the the number of RA resources. In [11, 12], the eNB is empowered with load estimation techniques to adjust the ACB factor in accordance with the optimal ACB in each RA procedure. In [13], a Proportional-Integral-Derivative (PID) controller is proposed to adjust the ACB factor in order to control the congestion level in the core network node. The authors of [14] apply the dynamic ACB factor to control the overload of MTCDs in both the radio access network and the core network of the LTE/LTE-A, simultaneously. 3GPP also specified the EAB for M2M communications, where individual applications can be controlled through broadcasting RA information called System Information Block (SIB) [4]. The performance of the EAB scheme for M2M communications and the optimal values of EAB parameters are analyzed in [15]. In addition to the EAB method, the specific backoff adjustment scheme for M2M communications has been introduced by 3GPP [7] where the requests of MTCDs are delayed in the case of overload. The authors in [16] investigated the throughput of the RA procedure in the LTE-A under different backoff timer. Although these works can control the congestion through barring the excessive access requests of MTCDs, they did not take into account the maximum acceptable delay of the barred MTCDs.

In the second category, the dynamic allocation of RA resources is introduced in [17], where the excessive

access requests are mitigated through allocating more RA resource. Authors in [18] used additional preambles to guarantee the access delay of emergency devices in an overload condition which improved the conventional RA procedure. In [6] the average number of successful transmissions increased through allocating more PUSCH to successfully detected preambles by the eNB. The number of contention resources is enhanced in [5] through a new codeword method. In this method, the MTC D selects one preamble on each RA sub-frame of a virtual frame. The virtual frame consists of some RA sub-frames that RA is performed over it. These approaches improve the throughput of the RA procedure at the cost of using more RA resources.

To decrease the access delay of MTC Ds without increasing RA resources, we have offered a multiple power level RA method in this paper. The proposed method is based on the capture effect in the RA which previously evaluated for the slotted ALOHA [19, 20, 21, 22, 23] and 802.11 [24] networks. We show that the access delay and the throughput of RA can be reduced and improved in the case of the overload through the proposed method.

3. SYSTEM MODEL AND PROBLEM STATEMENT

We consider the Frequency Division Duplexing (FDD) mode of the LTE-A system. In this mode, there are some Random Access Opportunities (RAO) in each frame in accordance with FDD configurations [25]. Each frame composed of ten subframes with 1ms duration each one. The number of RAOs in each frame determines the total number of RA resources in each frame as given by the multiplication of the number of PRACH subframes and the number of RA preambles. We use PRACH configuration index 6 as the typical configuration [7, 25], in which one PRACH subframe with 54 preambles is provided every 5ms. Notice that in this configuration, there are 54 preambles within one PRACH opportunity, the number of RAOs is equal to the number of preambles for each RA procedure.

Fig. 1 shows the system model considered in this paper. Event-driven M2M applications such as secure alarm, health emergency notification, the location update, and remote control have been considered. In the assumed traffic model, each idle MTC D triggers with probability α to transmit the early sensing data. We model the traffic of each MTC D by a two-state Markov chain that its states represent active and idle modes of MTC D operation, see Fig. 2. In Fig. 2, q_{S_L} refers to the probability of successfully transmitted requests among all active MTC Ds.

There are N_T MTC Ds in the system where some of them are active. The active MTC Ds include the new-triggered devices as well as the barred and unsuccessful devices from the previous RA procedure. The remaining MTC Ds which are in the idle state called inactive devices. To initiate the

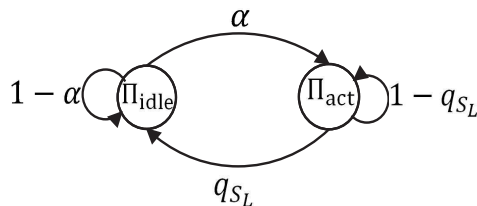


Figure 2. The traffic model of the MTC D

connection setup, each active MTC D will draw a random number between [0, 1] uniformly. The MTC D is allowed to start the RA procedure only if the drawing number is less than the ACB factor q_{ACB} announced by the eNB. The MTC D which passed the ACB check, referred as the contending MTC D in this paper, initiates the multiple power level RA procedure. We do not consider a limit on the number of retransmission attempts and the back-off interval before each transmission as in [26, 27]. That is, if the contending MTC D could not pass the RA procedure successfully, it continues the aforementioned process until its data is successfully received by the eNB.

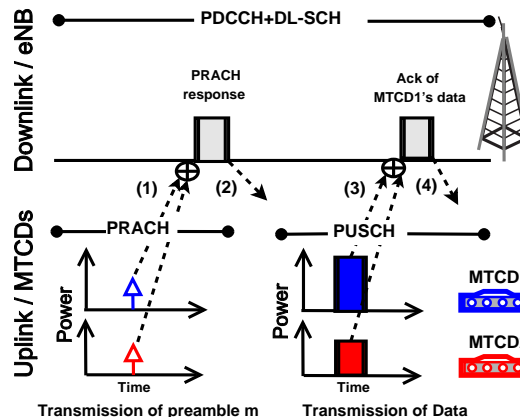


Figure 3. Multiple power level RA procedure

In this paper we consider a single cell in which all MTC Ds experience similar RA channel and configuration as in [19, 20, 21, 22, 23]. That is by comparing the SIRs, the powers of MTC Ds which transmit simultaneously is the key factor in deciding which MTC D can capture the granted uplink resources in the RA procedure.

The multiple power level RA procedure is shown in Fig. 3. The considered RA procedure consists of four steps as similar to the contention-based RA procedure in the LTE-A [3]. In the proposed multiple power level RA method, in contrast to [3], each MTC D which receives the Random Access Response (RAR) message in the access-granting step successfully, selects its transmission power according to a given probability mass function. The MTC D which its transmission power is high enough in comparison with the interference caused by the transmissions of other

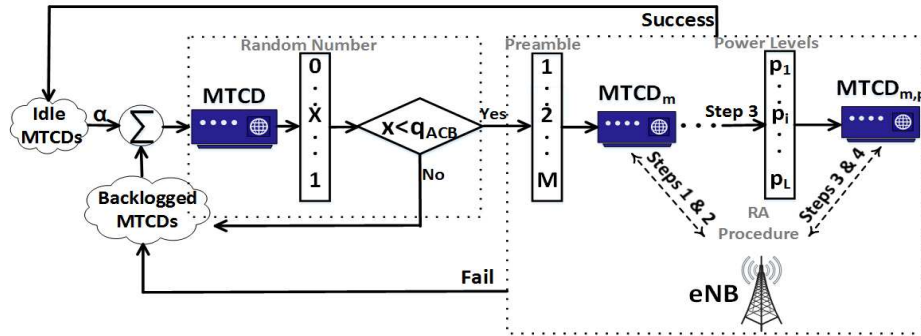


Figure 1. System model for multiple power level RA method.

MTCDs on the same RBs can capture the channel in the third step of the RA procedure. In what follows, the steps of the proposed multiple power level method will be explained.

In step 1, the contending MTCD randomly selects one preamble from the M2M dedicated RA preambles. We define the contending MTCDs which select the same preamble as co-tagged MTCDs. Notice that the eNB can decode the received preamble while it has been transmitted by the co-tagged MTCDs. However in this step, the eNB cannot differentiate whether the preamble is chosen by more than one MTC device [28, 29]. We do not consider the channel conditions and power ramping factor on successful preamble detection in the first step of the RA procedure. Hence, the preamble transmission power is adjusted according to the maximum transmit power, P_{CMAX} , as described by 3GPP [30]. The preamble transmission power is considered to be high enough that can be detected by the eNB. In the next step, the eNB replies the corresponding RAR messages through the Physical Downlink Control Channel (PDCCH) to acknowledge the received preambles (see step 2 in Fig. 3). The RAR message contains some information to inform the contending MTCD about the index of received preamble, timing advance command, and the dedicated PUSCH for transmitting message 3. We assume that in the considered massive access scenario, sufficient downlink and uplink resources are available in the second and third steps of the RA procedure if all dedicated M preambles are detected successfully. A comprehensive study of the constraints on the connection establishment in the LTE from downlink and uplink resources point of view is presented in [31].

In step 3, each contending MTCD successfully received the RAR from the eNB, selects its transmission power from a set of the candidate power levels, $\{p_1, p_2, \dots, p_L\}$, with their associated probabilities, $\{q_1, q_2, \dots, q_L\}$, to transmit message 3. Without loss of generality, we assume that $p_1 < p_2 < \dots < p_L$. Message 3 indicates the purpose of connection setup by the MTCD which may be data transmission [28, 29] or scheduled request [3]. In this step, the co-tagged MTCDs receive the same RAR through

the PDCCH and hence, transmit their data/scheduled-requests on the same PUSCH. In this case, in contrast to the preamble transmission in step 1, only one co-tagged MTCD can capture the channel if its transmission power is high enough in comparison with other co-tagged MTCDs' interferences. It is worth noting that the advantage of the power capture effect is also used in the power ramping technique which has been introduced by 3GPP working group [32]. At last in step 4, the eNB acknowledges the successfully received data/scheduled-requests of step 3, as shown in Fig. 3 for the $MTCD_1$ that capture the channel. Those contending MTCDs which did not receive the corresponding message in step 4, attempt at the next PRACH opportunity.

In the massive access scenario, the RA procedure suffers from the collisions caused by the simultaneous transmissions of message 3 via the same granted RBs when two or more MTCs select the same preamble in the RAR requests. Hence, two relevant capture models which are known as perfect model and SIR-based model are adopted for unconstrained and constrained energy budget scenarios in this paper, respectively, to evaluate the conditions that the simultaneous transmissions of message 3 in the eNB can be decoded. In the perfect model, $MTCD_i$ can transmit its data/scheduled-request among all other co-tagged $MTCD_j$, $j = 1, \dots, L$, $j \neq i$, successfully if $p_i > p_j$. While, in the SIR-based model, $MTCD_i$ can successfully accomplish the RA procedure if p_i be greater than the interference of other co-tagged MTCs, as:

$$p_i > \beta \left(\sum_{j=1, j \neq i}^L n_j p_j + (n_i - 1) p_i \right), \quad (1)$$

where β denotes the minimum required SIR which can be detected by the eNB, n_j and n_i refer to the number of co-tagged MTCs which select power level j and i , respectively. In the multiple power level RA method, the eNB broadcasts the PRACH configuration index, a vector of transmission powers, and power level selection probabilities in each RA procedure.

The objective of this paper is to increase the successful transmissions of MTCs while decreasing the access delay

in the case of the overload. That is by proper selection of barring factors and the corresponding power levels, we can determine the proper number of contending MTCDs in each power level in order to maximize the RA throughput. This causes the number of barring MTCDs and hence the average access delay of MTCDs to be decreased in comparison with the single power level RA procedure.

4. PROPOSED MULTIPLE POWER LEVEL RANDOM ACCESS METHOD

In this section, we first derive the RA throughput of the proposed method in the perfect capture model. In this paper, the RA throughput refers to the expected number of MTCDs which passes the RA procedure successfully in each PRACH opportunity. Then, the proposed method has been extended to the SIR-based model. We use an adaptive method to determine the ACB factor and the corresponding transmission powers according to the number of active MTCDs. Finally, we discuss how the proposed method can be deployed to serve MTCDs with different priorities in a real scenario. In what follows we exploit the capture effect at the eNB to improve the performance of the RA procedure and don't consider the successive interference cancelation which may also be used at the eNB.

4.1. Model 1: Perfect Capture Model

We first formulate the RA throughput of multiple power level RA procedure in the perfect capture model as an optimization problem and then the optimum value of the ACB factor and corresponding power levels selection probabilities are derived. By applying the optimum values of $q_i, i = 1, \dots, L$, the number of contending MTCDs can be balanced between different power levels to maximize the RA throughput. Therefore, the optimum values of barring factors can be obtained through finding the desired number of contending MTCDs in each power level.

Let S_i denote the RA throughput of the system with given i power levels. The RA throughput of the system with the single power level is determined by the success probability of n_1 given MTCDs multiplied by the number of preambles, M . In this case, the success probability of MTCDs is the probability that only one out of n_1 contending MTCDs selects each preamble, named m , and others do not. That is $\binom{n_1}{1}(\frac{1}{M})(1 - \frac{1}{M})^{n_1-1}$. Then, S_1 simplifies to (2).

$$S_1 = n_1 \left(1 - \frac{1}{M}\right)^{n_1-1}. \quad (2)$$

For a system with two power levels where $p_2 > p_1$, the RA throughput is the sum of the throughput of the first power level provided that there is not any interference from the second power level, and the throughput of the second power level, as:

$$S_2 = S_1 \left(1 - \frac{1}{M}\right)^{n_2} + n_2 \left(1 - \frac{1}{M}\right)^{n_2-1} \quad (3)$$

This process can be continued to find S_i . In summary, for a system with given L power levels, S_L is given by:

$$S_L = S_{L-1} \left(1 - \frac{1}{M}\right)^{n_L} + n_L \left(1 - \frac{1}{M}\right)^{n_L-1} \quad (4)$$

Assume that n_i MTCDs select power level i . We can find S_L as a function of $n_i, i = 1, \dots, L$, in a recursive manner as in (5).

$$S_L = \left(1 - \frac{1}{M}\right)^{\sum_{j=1}^{L-1} n_j} \rho_L \quad (5)$$

where $\rho_L = \sum_{i=1}^L n_i \left(1 - \frac{1}{M}\right)^{\sum_{j=i}^{L-1} n_j}$.

The objective is to find the optimal number of MTCDs which select power level i , n_i^* , such that S_L is maximized. The i^{th} component of the gradient of S_L with respect to n_i is given by (6).

$$\frac{\partial S_L}{\partial n_i} = \left(1 - \frac{1}{M}\right)^{\sum_{j=i}^{L-1} n_j-1} \left(1 - \ln\left(\frac{M}{M-1}\right)\rho_i\right) \quad (6)$$

Now, by setting (6) to zero, we can find n_i^* in a recursive manner as in (7).

$$n_i^* = \rho_i^* \left(1 - \left(1 - \frac{1}{M}\right)^{n_{i-1}^*}\right), \quad \rho_i^* = \frac{1}{\ln\left(\frac{M}{M-1}\right)} \quad (7)$$

where $n_1^* = \frac{1}{\ln\left(\frac{M}{M-1}\right)}$.

Lemma 4.1

$n_i^*, i = 1, \dots, L$ is the unique global optimal point of S_L in the perfect capture model.

Proof

See Appendix A. □

Also, the maximum RA throughput of a system with L power levels, S_L^* , can be obtained by replacing the optimal values of n_L and ρ_L , i.e. n_L^* and ρ_L^* , in (5).

According to (7), $1 - \left(1 - \frac{1}{M}\right)^{n_{i-1}^*}$ is a decreasing term of n_i^* and $n_i^* < n_{i-1}^*$. Therefore, for high enough values of i we will have $n_i \rightarrow 0$. That is S_L^* reaches to $\frac{M}{\ln\left(\frac{M}{M-1}\right)(M-1)} \simeq M$, which can be considered as the upper bound for S_L .

Let n_{act} be random variable denoting the total number of active MTCDs in each RA procedure. Assuming the traffic model of Fig. 2, the probability that each MTCD be in active state, Π_{act} , is given by (8). Also, the eNB can compute the expected value of the number of active MTCDs, $\mathbb{E}[n_{act}]$, in each RA opportunity.

$$\Pi_{act} = \frac{\alpha N_T - S_L}{\alpha N_T} \quad (8)$$

Now, by using (8), $\mathbb{E}[n_{act}]$ can be computed as in (9).

$$\mathbb{E}[n_{act}] = N_T \Pi_{act} \quad (9)$$

In an overload condition, the expected number of active MTCDs is greater than the sum of the desired number

of contenting MTCDs at all power levels, i.e., $\mathbb{E}[n_{act}] > \sum_{i=1}^L n_i^*$. In this case, q_{ACB} is used to block the excessive active MTCDs. Then, by obtaining the values of n_i^* and $\mathbb{E}[n_{act}]$ using (7) and (9), q_{ACB} and q_i can be computed from (10) and (11) respectively to sustain n_i in each power level near to its optimum value.

$$q_{ACB} = \min \left\{ 1, \frac{\sum_{i=1}^L n_i^*}{\mathbb{E}[n_{act}]} \right\} \quad (10)$$

$$q_i = \frac{n_i^*}{\sum_{i=1}^L n_i^*} \quad (11)$$

As a special case, it should be noted that if $L = 1$, using (10) and (11) we have $q_{ACB} = \frac{n_1^*}{\mathbb{E}[n_{act}]}$ and $q_1 = 1$, which is the traditional single power level ACB scheme. In a lightly loaded condition where $\alpha N_T < S_L^*$, we have $q_{ACB} = 1$. In this condition, by replacing n_i in (5) with $q_i \mathbb{E}[n_{act}]$, S_L can be found through solving (5), (8), and (9) numerically.

In the next step, we compute the average access delay of MTCDs using the obtained values for S_L and $\mathbb{E}[n_{act}]$ according to (5) and (9), respectively. In a system with L power levels, the access delay, d_L , for the MTCD accounts for the time duration between the first transmission attempt and the final successfully reception by the eNB. It is noted that each active MTCD continues the RA procedure to successfully transmit its data/scheduled-request in the next RA opportunities. Also, the probability of successful transmission, q_{S_L} , in each PRACH opportunity is the same and independent of previous attempts. Therefore, the number of retransmission attempts until the successful transmission is a random variable with geometric probability mass function that its expected value is given by $\frac{1}{q_{S_L}}$. Now, if T denotes the time interval between two consecutive PRACH opportunities, the average access delay, $\mathbb{E}[d_L]$, is given by the multiplication of T and $\frac{1}{q_{S_L}}$ as given in (12).

$$\mathbb{E}[d_L] = \frac{T}{q_{S_L}} \quad (12)$$

where the probability of successful transmission of the MTCD could be written as:

$$q_{S_L} = \frac{S_L}{\mathbb{E}[n_{act}]} \quad (13)$$

According to (12), it can be found that the average access delay can be decreased through enhancing the probability of successful transmission of MTCD in each RA procedure.

The perfect capture model describes the effectiveness of the proposed multiple power level RA procedure in a scenario in which the effects of MTCDs' energy budget on the successful transmission and access delay have not been considered. To consider the MTCDs' energy budget, the performance of the proposed method has been investigated for the SIR-based model in the next subsection.

4.2. Model 2: SIR-based Model

In this subsection, the RA throughput of the SIR-based capture model with L available power levels is computed. As mentioned earlier, a contending MTCD can transmit its data/scheduled-request successfully, if it can capture the channel among all other co-tagged MTCDs. In the SIR-based model, the channel is successfully captured by the MTCD with power level p_i if the following condition is satisfied.

$$p_i > \beta \left(\sum_{j=1}^{i-1} n_j p_j + (n_i - 1) p_i + \sum_{j=i+1}^L n_j p_j \right) \quad (14)$$

The first, second, and third terms in the right hand side of (14) are the interferences caused by the transmissions of lower, the same, and higher power levels of co-tagged MTCDs, respectively. Notice that when one or more co-tagged MTCDs with power level $j > i$ transmit the data/scheduled-request, transmissions of other co-tagged MTCDs with power level i will not be detected by the eNB as in the perfect capture model. The same also happens when $j = i$ but the number of MTCDs with power level i is greater than one, i.e., $n_i > 1$. However, for $j < i$, the number of co-tagged $MTCD_j$ determines the amount of incurred interference. This interference causes the probability of successfully decoding the transmitted data/scheduled-request from $MTCD_i$ at the eNB to be decreased. For a system with L power levels, in order to compute the probability of failure in the decoding of $MTCD_L$'s data/scheduled-request at the eNB, denoted by q_{K_L} , we continue as follows. Define K_L as a set of all vectors satisfying condition (15) [21]:

$$K_L = \left\{ \mathbf{k} = [k_1 k_2 \dots k_{L-1}] \mid \beta \sum_{j=1}^{L-1} k_j p_j > p_L \right\} \quad (15)$$

where $\mathbf{k} = [k_1, k_2, \dots, k_{L-1}]$ and k_i denote a specific vector of K_L and the number of MTCDs which use power level p_i respectively. It is noted that all MTCDs of \mathbf{k} select the same preamble in the first step of RA procedure. The occurrence probability of a specific \mathbf{k} , $q_{\mathbf{k}}$, can be obtained from (16).

$$q_{\mathbf{k}} = \prod_{j=1}^{L-1} f(k_j; n_j, \frac{1}{M}) \quad (16)$$

where $f(k_j; n_j, \frac{1}{M}) = \binom{n_j}{k_j} (\frac{1}{M})^{k_j} (1 - \frac{1}{M})^{n_j - k_j}$ is the binomial probability mass function. Since q_{K_L} is the probability of all vectors like \mathbf{k} which satisfying condition (15), this probability is equivalent to the sum of $q_{\mathbf{k}}$ as:

$$q_{K_L} = \sum_{\mathbf{k} \in K_L} q_{\mathbf{k}} \quad (17)$$

Now, by applying (17), the throughput in (4) can be found for the SIR-based model as given by (18).

$$S_L = S_{L-1} \left(1 - \frac{1}{M}\right)^{n_L} + n_L \left(1 - \frac{1}{M}\right)^{n_L-1} (1 - q_{K_L}) \quad (18)$$

$1 - q_{K_L}$ in (18) determines the probability of successfully decoding the transmitted data/scheduled-request from MTCD with power L at the eNB. According to (18), the first term is the throughput from transmissions of all co-tagged $MTCD_i$ for $i < L$. The second term indicates the throughput of $MTCD_L$'s transmission while the imposed interference from other co-tagged $MTCD_s$ that $i < L$ is β times lower than the transmission power of $MTCD_L$. According to (18), S_L can be found as the function of $n_i, i = 1, \dots, L$, and q_{K_i} in a recursive manner as in (19).

$$S_L = \sum_{i=1}^L n_i \left(1 - \frac{1}{M}\right)^{\sum_{j=i}^L n_j - 1} (1 - q_{K_i}) \quad (19)$$

Since S_L is a function of both p_i and n_i , we need to find the optimum values of p_i and n_i to maximize S_L . High transmission power or greater number of contending MTCDs in each power level leads to more energy consumption of MTCDs. To consider the energy efficiency issue, the MTCD's energy budget in each RA procedure can be bounded. Let \mathcal{E} be the random variable denoting the energy consumption of the MTCD in each RA procedure. We define $\mathbb{E}[\mathcal{E}]$ as the expected energy consumption in each RA procedure as given by (20).

$$\mathbb{E}[\mathcal{E}] = \frac{\sum_{i=1}^L n_i \mathcal{E}_i}{\sum_{i=1}^L n_i} \quad (20)$$

where \mathcal{E}_i is the energy consumption of the MTCD with power level p_i and is obtained through the multiplication of p_i and the duration of one PRACH opportunity, T_1 , i.e., $\mathcal{E}_i = p_i T_1$. Since the preamble transmission power is considered to be constant for all MTCDs and for all RA opportunities, we just consider the energy consumption of transmitting message 3 in (20) and ignore the energy usage of the first step of RA procedure.

Now, the problem of maximizing S_L subject to the expected energy consumption constraint can be formulated as follows:

$$\max_{n_1, \dots, n_L, p_2, \dots, p_L} S_L \quad (21)$$

$$s.t. \quad p_{i-1} \leq p_i, \quad i = 2, 3, \dots, L, \quad (22)$$

$$\mathbb{E}[\mathcal{E}] \leq \mathcal{E}_0 \quad (23)$$

where (22) states that the amount of transmission power is increased by increasing the power level index. Constraint (23) ensures that the expected value of MTCDs' energy consumption is not greater than the determined threshold, \mathcal{E}_0 . By increasing \mathcal{E}_0 , the differences between power levels are increased. This causes q_{K_L} to be decreased and hence, S_L to be increased. For a high enough value of \mathcal{E}_0 , there are not any interference from the transmissions of lower

power levels, i.e., $q_{K_i} = 0, i = 2, \dots, L$. In this case, n_i is equal to what has been obtained in (7), and the RA throughput of the system is reached to the throughput of the perfect capture model. For the minimum value of \mathcal{E}_0 , i.e., $\mathcal{E}_0 = p_1 T_1$, by replacing (20) in constraint (23), we have $n_i = 0$ for $i > 1$; which concludes the single power level RA procedure.

For other values of \mathcal{E}_0 , variables that should be determined in (21)-(23) are $n_1 \dots n_L$ and $p_2 \dots p_L$, as the desired integer and real positive numbers respectively. The value of p_1 is considered to be as the same as the preamble transmission power. Since the formulated problem in (21)-(23) is a nonlinear problem with mixed discrete and continuous variables, we use Genetic algorithm to solve it in an intelligent exhaustive search manner.

In the following, the relationship between $n_i, i = 1, \dots, L$ and $p_i, i = 1, \dots, L$, is illustrated for the special case of $L = 2$ in (21)-(23). In this case, from (15) and (16) we have $k_1 \geq \frac{p_2}{\beta p_1}$ and $q_{K_2} = f(k_1; n_1, \frac{1}{M})$, respectively. Hence, using (17), the probability of failure in the decoding of $MTCD_2$'s data/scheduled-request at the eNB can be computed as given in (24).

$$q_{K_2} = \sum_{k_1 = \frac{p_2}{\beta p_1}}^{n_1} f(k_1; n_1, \frac{1}{M}) \quad (24)$$

Notice that k_1 in (24) is an integer number and hence p_2 can be represented by $p_2 = \beta c p_1$ where c is an integer. If p_2 has been replaced by $\beta c p_1$ in (24), it can be found that $1 - q_{K_2}$ is equivalent to $Pr(k_1 \leq c)$; which is the Cumulative Distribution Function (CDF) of binomial distribution. The CDF of binomial distribution, $F(c; n_1, \frac{1}{M})$, can be substituted with the regularized incomplete beta function, $I_{\frac{c}{M}}(n_1 - c, c + 1)$, where $I_x(a, b)$ is defined as $\frac{B(x; a, b)}{B(a, b)}$ and $B(x; a, b)$ and $B(a, b)$ are incomplete and complete beta functions respectively [33]. Therefore, the problem in (21)-(23) can be represented for $L = 2$ by substituting p_2 and $1 - q_{K_2}$ with $c\beta p_1$ and $I_{\frac{c}{M}}(n_1 - c, c + 1)$ respectively, as follows:

$$\max_{n_1, n_2, c} S_2 = n_1 \left(1 - \frac{1}{M}\right)^{n_1 + n_2 - 1} + n_2 \left(1 - \frac{1}{M}\right)^{n_2 - 1} \mathbf{I}_{\frac{c}{M}}(n_1 - c, 1 + c) \quad (25)$$

$$s.t. \quad \frac{T(n_1 p_1 + n_2 c \beta p_1)}{n_1 + n_2} \leq \mathcal{E}_0, \quad (26)$$

where n_1, n_2 , and c are integer numbers. According to the property of the regularized incomplete beta function, it can be inferred that $\mathbf{I}_{\frac{c}{M}}(n_1 - c, 1 + c)$ is monotonically increasing function of c and hence of p_2 , while it is monotonically decreasing of n_1 . This means that the imposed interferences from $MTCD_s$'s transmissions can be mitigated by decreasing the number of contending $MTCD_s$ or increasing the transmission power p_2 . Also, according to the objective function in (25), the value of

p_2 only determines the amount of incurred interference. Therefore, the RA throughput can be enhanced by increasing the transmission power p_2 . In order to increase the transmission power p_2 , we can search for the maximum value of c satisfying constraint (26) with given values of n_1 and n_2 . Therefore, the objective function in (25) can be expressed in terms of two variables n_1 and n_2 ; which limit the search space to a small feasible region. Due to the limited search region, the optimization problem in (25)-(26) can be solved by searching all possible values of n_1 and n_2 , $n_1, n_2 \in \{1, \dots, M\}$. After solving the optimization problem, the values of q_{ACB} , q_i , and $\mathbb{E}[d_L]$ can be computed using (10), (11), and (12) respectively.

4.3. Priority based multiple power level RA

The multiple power level scheme can be deployed to prioritize some MTCDs against others. In this subsection, we discuss the required conditions to guarantee the priority of MTCD with a higher power level against the transmissions of the lower power levels in the RA procedure while at the same time the RA throughput is maximized.

Let $S_{L,i}$ represent the expected number of successfully transmitted requests at the i^{th} level of a system with given L power levels. It can be inferred from (19) that $S_{L,i}$ is given by:

$$S_{L,i} = n_i \left(1 - \frac{1}{M}\right)^{\sum_{j=i}^L n_j - 1} (1 - q_{K_i}) \quad (27)$$

According to (27) for $q_{K_i} = 0$ and $n_i = n_i^*$, $S_{L,i}$ would be equal to the number of successfully transmitted requests from the i^{th} power level in the perfect capture model at the optimal RA throughput. In this case, $S_{L,i}$ is denoted by $S_{L,i}^*$.

Due to the various obtained throughput for different power levels in (27), the proposed RA procedure can be used to discriminate among MTCDs with different priorities. Since MTCDs with higher power levels consume more energy in comparison to MTCDs with lower power levels, in what follows we find the required condition to guarantee the priority of these MTCDs in the RA procedure. We continue this study for a system with two power levels, however, it can be extended to deal with multiple power level system. In order to guarantee the number of successfully transmitted requests of the second power level to be more than a predefined threshold like Γ_0 , the optimization problem in (25)-(26) can be revised by considering the condition of $S_{2,2} \geq \Gamma_0$ as follows:

$$\max_{n_1, n_2, c} S_2 = n_1 \left(1 - \frac{1}{M}\right)^{n_1 + n_2 - 1} + n_2 \left(1 - \frac{1}{M}\right)^{n_2 - 1} \mathbf{I}_{\frac{M-1}{M}}(n_1 - c, 1 + c) \quad (28)$$

$$s.t. \quad \frac{T(n_1 p_1 + n_2 c \beta p_1)}{n_1 + n_2} \leq \mathcal{E}_0, \quad (29)$$

$$n_2 \left(1 - \frac{1}{M}\right)^{n_2 - 1} \mathbf{I}_{\frac{M-1}{M}}(n_1 - c, 1 + c) \geq \Gamma_0, \quad (30)$$

where $S_{2,1}$ and $S_{2,2}$ are $n_1 \left(1 - \frac{1}{M}\right)^{n_1 + n_2 - 1}$ and $n_2 \left(1 - \frac{1}{M}\right)^{n_2 - 1} \mathbf{I}_{\frac{M-1}{M}}(n_1 - c, 1 + c)$ respectively. The optimization problem in (28)-(30) can be solved numerically to find the optimum values of n_1 and n_2 at feasible points. Notice that the optimum value of c is obtained by replacing different values of n_1 and n_2 in (29) to find the maximum value of c which satisfy this inequality. This optimization problem can be simplified to the perfect capture model when \mathcal{E}_0 is high enough. Since in this case S_2 has a single global maximum, see Lemma 1, the RA throughput of the system for $\Gamma_0 < S_{2,2}^*$ reaches to S_L^* and the optimum values of n_1 and n_2 are computed using (7). If $\Gamma_0 > S_{2,2}^*$, the optimum value of n_2 is computed through solving $n_2 \left(1 - \frac{1}{M}\right)^{n_2 - 1} = \Gamma_0$, numerically. Then, the optimum value of n_1 can be found by substituting the optimum value of n_2 into the objective function in (28) and searching for all possible values of n_1 which maximize (28). It is noted that the maximum value of Γ_0 equals to the RA throughput of the single power level system which is S_1^* .

Notice that considering the priority of MTCDs with higher power levels may lead to the decrease in the number of total successfully transmitted requests in the system as expected at the optimal point. This happens when the number of transmitted requests from the higher power levels is greater than its optimal value.

5. PERFORMANCE EVALUATION

In this section, the performance of the proposed multiple power level RA procedure has been compared with the single power level RA or the traditional ACB scheme by simulation and analysis. The results discussed in four subsections including: the perfect capture model, the SIR-based capture model, the priority point of view, and the implementation issues. We consider a scenario in which the eNB broadcasts the required parameters for the RA procedure, i.e., q_{ACB} and q_i . Then, each active MTCD initiates the RA procedure with probability q_{ACB} . In the considered RA procedure, each contending MTCD selects the m^{th} preamble in the first step and the i^{th} power level in the third step of RA procedure with probability $\frac{1}{M}$ and q_i respectively, to transmit the request to the eNB. Values of q_{ACB} and q_i are computed according to what has been discussed for the perfect capture model and the SIR-based capture model in subsections 4.1 and 4.2, respectively.

In the simulated scenario, we assume that the arrival probability of MTCDs is 0.003 and the eNB is able to estimate the number of active MTCDs in each RA procedure. We should note that since each MTCD continues its access attempts until it could successfully transmit its request, the number of access attempting requests in each RA procedure is much greater than the expected new access attempts. The simulation results are averaged over 5000 RA runs. The values of the simulation parameters are summarized in Table 1.

Table I. System parameters

Parameter	Details	Value
M	Number of preambles	54
p_1	Reference Power level for L_1	23dBm
α	The arrival probability of MTCs	0.003
T	time interval between two PRACH opportunities	5ms
T_1	Duration of one RA procedure	1ms

In what follows, the performance of the proposed multiple power level RA method is evaluated in terms of the RA throughput and the average access delay of MTCs. It is shown that the performance metrics can be improved at the cost of slightly increasing the energy consumption of MTCs.

5.1. Performance results of the perfect capture model

In this subsection, the performance of the proposed RA procedure has been investigated for the perfect capture model. In Fig. 4 and its corresponding contour curves in Fig. 5, the RA throughput of the system with two power levels for different number of contending MTCs at each power level are depicted. For analytical results, the RA throughput is obtained by substituting values of n_1 and n_2 , $n_1, n_2 \in \{5, 10, \dots, M\}$, in (5). The maximum value of RA throughput happens at the values which are expected by (7).

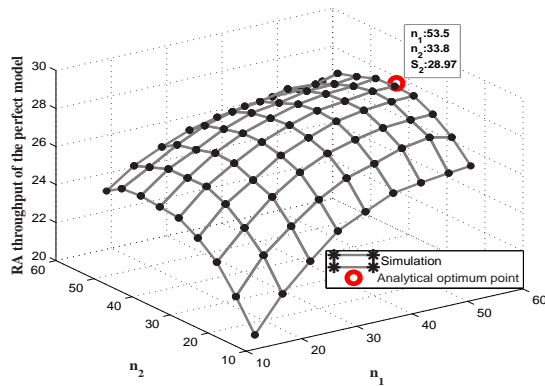


Figure 4. The throughput of two power level RA procedure for different values of n_1 and n_2 when $N_T = 15000$

In Fig. 6, the throughput of the proposed RA procedure in the perfect capture model against different number of MTCs is shown for $L = 1, 2, 3, 4$. For the analytical results, the RA throughput for different values of L can be found according to what has been discussed in section

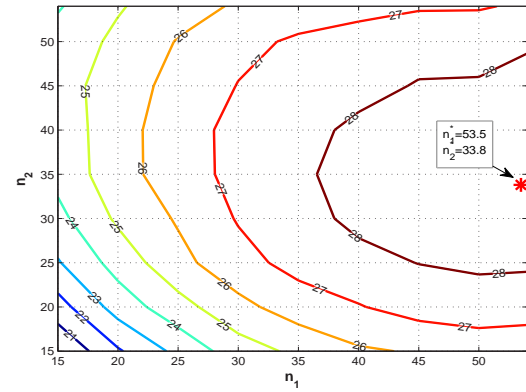


Figure 5. Contour curves of Fig. 4

4.1. We find from Fig. 6 that S_L is greater than S_{L-1} , emphasizes that the achievable RA throughput is increased with the number of power levels. In addition, S_L in each power level has been increased by increasing the number of MTCs until it reaches to its maximum value for each power level. As previously mentioned, the maximum RA throughput of each power level happens in an overload condition where $N_T > \frac{S_L^*}{\alpha}$. If $N_T < \frac{S_L^*}{\alpha}$, S_L has a value between S_{L-1}^* and S_L^* as shown in Fig. 6. The circle markers in Fig. 6 show the values of N_T where $N_T = \frac{S_L^*}{\alpha}$ for $L = 2, 3, 4$. These values of N_T can be used by the eNB to determine the number of power levels in accordance with the total number of MTCs. This means that in a lightly loaded condition, the proposed RA procedure can be switched to the lower power levels in order to decrease the MTCs' energy consumption. From the resource efficiency point of view, we can notice to the ratio of the RA throughput values to the total number of possible accommodated requests using $M = 54$ preambles. According to Fig. 6, the resource efficiency is equal to 0.37 for $L = 1$, 0.54 for $L = 2$, 0.63 for $L = 3$, and 0.69 for $L = 4$.

Fig. 7 compares the average access delay of MTCs in the perfect capture model for different values of L , $1 \sim 4$. In this figure, the value of $\mathbb{E}[d_L]$ is derived using (12). We find from Fig. 7 that $\mathbb{E}[d_L]$ increases linearly when the total number of MTCs is increased. However, the rate of increasing for $L = 1$ is greater than that for $L = 2, 3, 4$. This indicates that by applying more power levels in an overload condition, the RA delay can be mitigated compared to the traditional single power level RA scheme.

5.2. Performance results of the SIR-based capture model

Here, the performance of the proposed method while bounding the energy budget of MTCs is investigated for the SIR-based capture model. In the following results, the optimum values of RA parameters, i.e., n_1, \dots, n_L and p_2, \dots, p_L , are computed by solving (21)-(23). We use

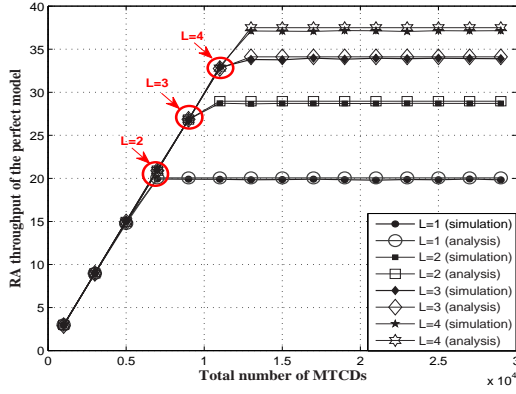


Figure 6. The throughput of the RA procedure in the perfect capture model against different values of N_T for $L = 1, 2, 3, 4$

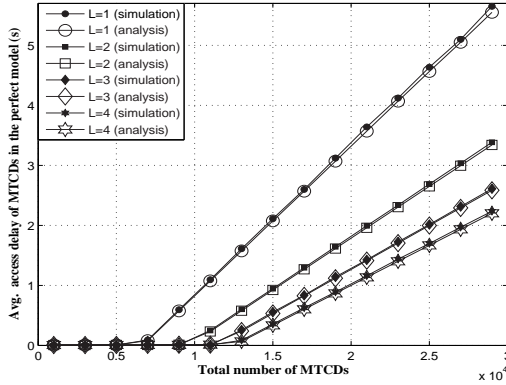


Figure 7. The average access delay of each MTCD in the perfect capture model against different values of N_T for $L = 1, 2, 3, 4$

the genetic algorithm to solve the optimization problem in (21)-(23). The average access delay for this model is computed using (12).

The throughput of the proposed method against different values of energy budget is shown in Fig. 8 for $L = 2, 3, 4$ and $\beta = 1.2$. This figure shows that for the minimum value of \mathcal{E}_0 , i.e., $T_1 p_1 = 0.19mJ$, the RA throughput of the system with 2, 3, and 4 power levels are the same with a single power level scheme. Also, this situation happens for $\mathcal{E}_0 = 0.25mJ$ where the RA throughput of the system with 4 power levels is equal to the system with 3 power levels. On the other side, the RA throughput can be increased up to its maximum value through more energy consumption. The maximum value of S_L in the SIR-based capture model has the same value for the perfect capture model which is demonstrated by the dashed lines in Fig. 8.

The average access delay of MTCDs against different values of \mathcal{E}_0 for $L = 2, 3, 4$, $\beta = 1.2$, and $N_T = 15000$ is shown in Fig. 9. According to this figure, $\mathbb{E}[d_L]$ is decreased at the cost of more energy consumption. In

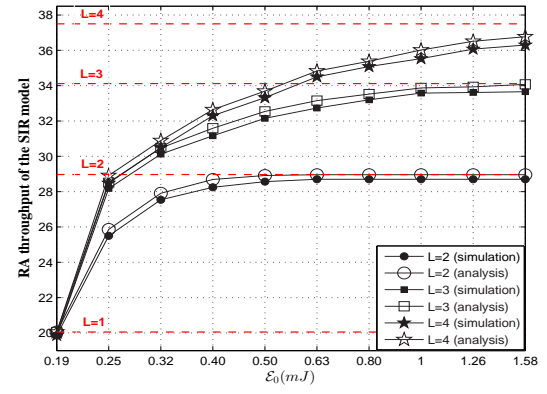


Figure 8. The throughput of the RA procedure in the SIR-based capture model against different values of \mathcal{E}_0 for $N_T = 15000$, $\beta = 1.2$, and $L = 1, 2, 3, 4$

addition, for a given MTCD's energy budget, the average access delay is decreased by increasing the number of power levels.

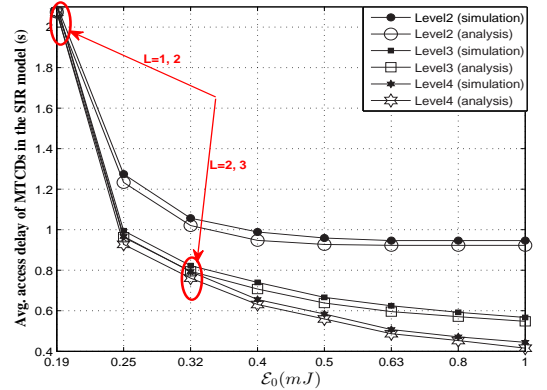


Figure 9. The average access delay of the MTCD in the SIR-based capture model against different values of \mathcal{E}_0 for $N_T = 15000$, $\beta = 1.2$, and $L = 1, 2, 3, 4$

In Fig. 10, the average access delay of the system with two power levels against different values of \mathcal{E}_0 is shown for $\beta = 1.2, 2.2, 3.2$. As expected for the lower values of β and when \mathcal{E}_0 is high enough, the average access delay is decreased since each co-tagged MTCD has higher chance to capture the channel in the presence of other co-tagged MTCDs' interferences. Also, according to (20) and (23), for $\mathcal{E}_0 = p_1 T_1 = 0.19mJ$, the optimum value of n_2 would be equal to zero and hence, the value of $\mathbb{E}[d_2]$ reaches to the average access delay of the system with single power level, as it is shown in Fig. 10. However, for the high enough values of \mathcal{E}_0 , the successful transmission probability of MTCDs with the second power level is increased that leads to decrease in the value of $\mathbb{E}[d_2]$ and tends to its optimal value at the perfect capture model. The reason is that in

this case the interference caused by the transmissions from the first power level on $MTCD_{S_2}$ could be overcome. The maximum and the minimum values of $\mathbb{E}[d_2]$ are shown with circle markers in Fig. 10.

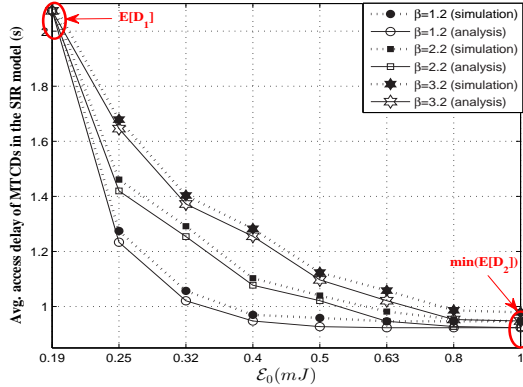


Figure 10. The average access delay of the MTCD in the SIR-based capture model against different values of \mathcal{E}_0 for $N_T = 15000$ and $\beta = 1.2, 2.2, 3.2$

5.3. Performance results of the priority based multiple power level RA method

In this section, it is shown that the proposed method can be used to provide different priorities for MTCDs with distinct two power levels. In this simulation, the optimum values of n_1 and n_2 have been obtained by solving (28)-(30) numerically. Also, for the analytical results, the number of successfully transmitted requests of each power level is computed using (27).

The average number of successfully transmitted data/scheduled-requests of each power level in the SIR-based capture model is shown in Fig. 11 for $L = 2$ against different values of \mathcal{E}_0 . In this figure, the value of Γ_0 is considered to be 16. According to this figure, we find that S_2 is an increasing function of \mathcal{E}_0 as it is expected. Also, we note that the values of $S_{2,1}$ and $S_{2,2}$ are not necessarily an increasing function of \mathcal{E}_0 at the optimum RA throughput. Furthermore, we note that $S_{2,2}$ is greater than the determined threshold which indicates the priority of MTCDs of the second power level against MTCDs of the first power level in the RA. In addition, for the high enough values of \mathcal{E}_0 , $S_{2,1}$ and $S_{2,2}$ are reached to their optimal values in the perfect capture model, $S_{2,1}^*$ and $S_{2,2}^*$.

In Fig. 12, we show the effect of Γ_0 on the number of successfully decoded requests from the first and second power levels of the system with two power levels. We find that for $\Gamma_0 < S_{2,2}^*$, i.e., $\Gamma_0 < 18.32$, the values of $S_{2,1}$ and $S_{2,2}$ are equal to their expected optimal values, $S_{2,1}^*$ and $S_{2,2}^*$ respectively, which leads to the maximum RA throughput. In this case, the value of Γ_0 does not impose additional constraint on the problem. However, if $\Gamma_0 > 18.32$, the value of $S_{2,2}$ is increased linearly by

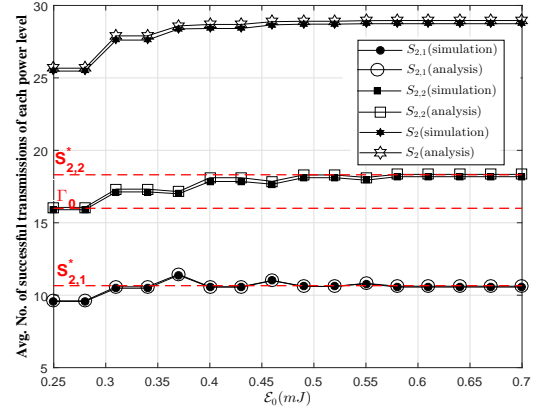


Figure 11. The average number of successfully transmitted requests of each power level for the system with two power levels against different values of \mathcal{E}_0 for $N_T = 15000$, $\beta = 1.2$, and $\Gamma_0 = 16$

increasing Γ_0 to ensure that the number of successfully transmitted requests from the second power level meet the imposed constraint. In this case the number of successfully transmitted requests from the first power level is decreased.

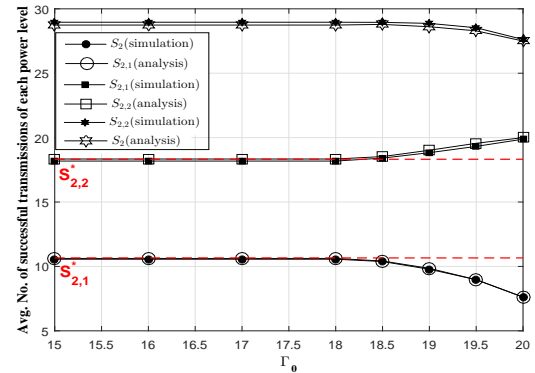


Figure 12. The average number of successfully transmitted requests of each power level for a system with two power levels against different values of Γ_0 for $N_T = 15000$, $\beta = 1.2$, and $\mathcal{E}_0 = 0.6mJ$

5.4. Implementation issues

In the analysis of the proposed multiple power level RA scheme we consider some simplifying assumptions. In this subsection, we provide the simulation results of the multiple power level RA scheme considering some implementation issues. In these simulations, we consider the maximum allowable number of MTCDs' retransmission attempts, the probability of successful preamble detection, the accuracy of the estimator at the

eNB, and the constraints on connection establishment in the LTE.

A. Maximum number of retransmission attempts

According to the 3GPP specifications, each collided MTCD should reattempt the RA procedure after a random backoff time if the maximum number of retransmission attempts has not been reached [3]. In our analysis we do not consider a limit on the number of retransmission attempts and the back-off time before each transmission. In what follows, we provide the simulation results of the proposed method against different values of the maximum number of retransmission attempts which is denoted by R_{max} as in [26].

We consider a scenario of the perfect capture model in which each collided MTCD will wait for a random number of RA opportunities that selected according to a uniform probability distribution between 0 and W_{max} . The value of W_{max} is set to be 20 RA opportunities. Also, if the maximum number of retransmissions attempts is reached, the collided MTCD will give up the RA procedure and will return to the idle state until new data arrival. Notice that each collided MTCD will become active after a backoff duration and perform the ACB check to participate in the RA procedure according to what has been discussed in section 3.

The average access delay of MTCDs against different values of R_{max} for $L = 1$ and $L = 2$ is shown in Fig. 13. As it is expected, by increasing R_{max} , most of the MTCDs remain backlogged and hence experience more access delay as it is shown for $\mathbb{E}[d_1]$ and $\mathbb{E}[d_2]$ in Fig. 13. The maximum MTCDs' access delay happens in the case where there is no limit for retransmission attempts, i.e., $R_{max} = \infty$. In this case, the values of $\mathbb{E}[d_1]$ and $\mathbb{E}[d_2]$ can be computed using (12) as 2.07 and 0.92 respectively; which are demonstrated by the dashed lines in Fig. 13. When $R_{max} = 0$, the collided MTCDs do not retry to transmit their data/scheduled-requests. This causes the contending MTCDs remain active with probability $1 - p_{ACB}$ and return to the idle state with probability p_{ACB} . Hence, by replacing q_{S_L} with q_{ACB} , the probability that each MTCD be in active state, Π_{act} , would be equal to $\frac{\alpha}{\alpha + q_{ACB}}$. Then, by substituting the value of Π_{act} in (9) and by solving (9) and (10), we can find the values of q_{ACB} and $\mathbb{E}[n_{act}]$ as 1 and 44.86 for both scenarios of $L = 1$ and $L = 2$. In this case, the expected number of contending MTCDs is equal to $\mathbb{E}[n_{act}]$ for $L = 1$ and $L = 2$ because of $q_{ACB} = 1$. Since $q_{ACB} = 1$ and $R_{max} = 0$, there is no backlogged MTCDs and the average access delay is equal to the time period of one PRACH subframe, i.e., $\mathbb{E}[d_L] = 5ms, L = 1, 2$. Also, it is worth to mention that the average access delay in a system with two power levels is less than the single power level scheme.

B. The effect of estimation and unsuccessful preamble detection at the eNB

So far, it is assumed that the eNB knows the number of active MTCDs in each PRACH opportunity and there is no error in detecting the received preambles by the eNB at

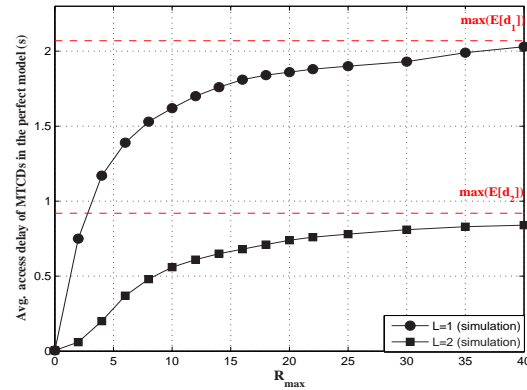


Figure 13. The average access delay of each MTCD in the perfect capture model against different values of R_{max} for $L = 1, 2$ and $N_T = 15000$

the first step of the RA procedure. However, in a practical scenario of M2M communications over LTE network, the eNB may not be able to detect all transmitted preambles by the MTCDs and should estimate the number of active MTCDs in each PRACH opportunity. Regarding these implementation issues, we have simulated and compared the RA throughput of the single power level and two power level schemes for three different scenarios: the RA with the perfect estimator and detector (ideal scenario), the RA with the imperfect detector, and the RA with the imperfect estimator. Simulation results have been shown in Fig. 14 for $R_{max} = \infty, W_{max} = 0$.

In the imperfect detection scenario, we assume that the eNB cannot detect the transmitted preambles by the MTCDs with probability q_e . Fig. 14 shows that at the detection error of $q_e = 0.2$, the achieved throughput of both single power level and two power level schemes are almost %20 less than their corresponding ideal throughput. We note that in the proposed multiple power level RA method, only one co-tagged MTCDs may accomplish the RA procedure. Hence, each detected preamble by the eNB may imply just one successful transmission at the end of RA procedure. Therefore, for large number of MTCDs, the error in preamble detection leads to the reduction in the RA throughput proportionally. For $N_T < 5000$, due to the lower number of selected preambles, there is not a significant difference between the ideal throughput and the other scenarios for $q_e = 0.2$.

To investigate the effect of estimating the number of active MTCDs at the eNB, we use the estimation technique of [27] in each RA procedure. In this technique, at the first, the eNB counts the number of idle preambles in the i^{th} PRACH opportunity and divides it by M to compute the probability that one preamble remains idle, $q_{idle,i}$. Then, by considering the value of $q_{idle,i}$, the number of contending MTCDs which is denoted by \hat{C}_i , can be computed as follows [27]:

$$\hat{C}_i = \frac{\ln(\tilde{q}_{idle,i})}{\ln\left(\frac{M-1}{M}\right)}$$

Now, the eNB can compute the number of active MTCDs in the $(i + 1)^{th}$ PRACH opportunity from \hat{C}_i and $q_{ACB,i}$ as follows [27]:

$$\hat{n}_{act,i+1} = \frac{\hat{C}_i}{q_{ACB,i}}$$

Also, according to (10) and by using the value of $\hat{n}_{act,i+1}$, the eNB updates the ACB factor in the $(i + 1)^{th}$ PRACH opportunity as given by:

$$q_{ACB,i+1} = \min\left\{1, \frac{\sum_{i=1}^L n_i^*}{\hat{n}_{act,i+1}}\right\}$$

The number of contending MTCDs can be controlled by broadcasting the updated value of q_{ACB} by the eNB in each RA procedure after estimation. As it is shown in Fig. 14, the RA throughput of the single and two power level schemes using this estimation technique follow the corresponding ideal scenario where the proposed multiple power level scheme outperforms the single power one.

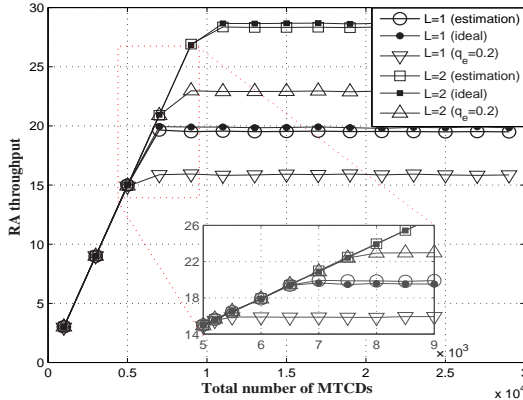


Figure 14. The RA throughput of the perfect capture model against different values of N_T for three considered scenarios when $W_{max} = 0$, $R_{max} = \infty$, and $L = 1, 2$

C. Constraints on connection establishment

Connection establishment in the LTE suffers from the limited amount of the resources available in downlink and uplink. This causes all contending MTCDs which successfully pass the first step of RA procedure, can not be served by the eNB. That is, there is not sufficient resources in the PUSCH, PDCCH, and Physical Downlink Shared Channel (PDSCH) for the traffic generated from the selected preambles by the MTCDs. To show the performance of the multiple power level RA method when there are constraints on the resources of uplink and downlink, we consider a simple scenario of the perfect capture model in which the number of contending MTCDs in each PRACH opportunity is limited in

accordance with the available resources. Let λ_0 denote the allowable number of contending MTCDs in each PRACH opportunity that can be served by the eNB. In order to sustain the number of contending MTCDs around λ_0 , it is assumed that the eNB computes the ACB factor using the value of λ_0 , and broadcasts it in each PRACH opportunity. Therefore, by considering λ_0 , q_{ACB} would be equal to $\min\left\{1, \frac{\lambda_0}{\mathbb{E}[n_{act}]}\right\}$. We do not consider the available number of preambles for computing the value of q_{ACB} . The parameters of this simulation are as follows: $N_T = 15000$, $M = 54$, $R_{max} = \infty$, $W_{max} = 0$.

Fig. 15 shows the RA throughput of the system with $L = 1, 2, 3$ power levels against different values of λ_0 . Notice that the RA throughput of the system with L power levels can be computed by replacing n_i in (5) with the multiplication of q_i and the number of contending MTCDs, i.e., $q_{ACB}\mathbb{E}[n_{act}]$. As it is shown in Fig. 15, the RA throughput of the system with two and three power levels outperform the single power level scheme when λ_0 is almost greater than 15. Also, as it is expected, the maximum RA throughput of the system with L power levels happens at the values that the total number of contending MTCDs is equal to $\sum_{i=1}^L n_i^*$; which are equal to 53.5, 87.31, and 112.37 for $L = 1, L = 2$, and $L = 3$.

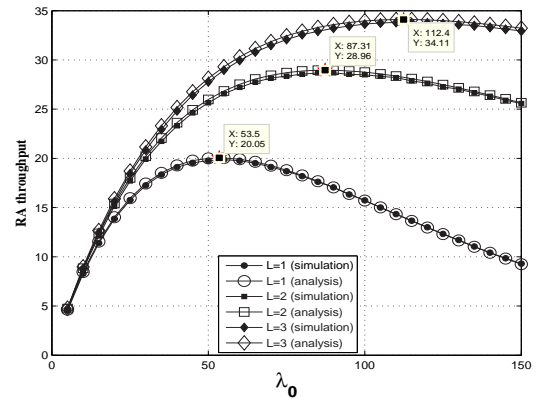


Figure 15. The RA throughput of the perfect capture model against different values of λ_0 for $N_T = 15000$, $M = 54$, $R_{max} = \infty$, $W_{max} = 0$, and $L = 1, 2, 3$

6. CONCLUSION

We proposed the multiple power level RA method to improve the performance of the RA throughput of M2M communications in the LTE/LTE-A network. At first, the optimum selection probability of each power level is derived based on the perfect capture model. Then, by considering the constrained energy budget of MTCDs, we extend the results for the SIR-based capture model. The proposed method has been evaluated for different numbers of MTCDs and different values of MTCD's

energy budget in the perfect capture model and the SIR-based capture model, by simulation. Moreover, we show that by considering the required condition, the proposed method can be used to prioritize the access of MTCDs. The results show that the multiple power level RA method can enhance the average number of successful transmissions and decrease the average access delay of MTCDs at the cost of more energy consumption of MTCDs and more computations at the eNB. These advantages of the multiple power level RA method makes it suitable for emergency situations such as the power grid blackout. For future work, we will investigate the effects of RA channel properties, i.e., noise and fading effects, on successful transmissions at each power level.

A. THE PROOF OF LEMMA 1

This Lemma is proved by checking whether $n_i^*, i = 1, \dots, L$ is, in fact, the global optimum point of function S_L . It is clear from (5) that S_L is a continuous function of n_i on the closed and bounded domain $\mathbf{dom} S_L = \{n_i | n_i \in (0, M)\}$. Therefore, according to the extreme value theorem, there is a global maximum and global minimum for S_L in the interior or the boundary of $\mathbf{dom} S_L$ [34]. By setting the gradient of S_L in (6) to zero, we can find the extremum points of S_L in the interior of $\mathbf{dom} S_L$. It is clear from (6) that $n_i^*, i = 1, \dots, L$ is the only extremum point of S_L in the interior of its domain. Now, to show that $n_i^*, i = 1, \dots, L$ is actually the global maximum, we check the value of S_L at the boundary $\mathbf{dom} S_L$, i.e., 0 and M , to be lower than S_L^* .

To this end, it is assumed that $n_1^*, n_2^*, \dots, n_{L-1}^*$ are the optimal values of S_{L-1} ; which means that $S_{L-1}^* > S_{L-1}$ for $n_i \in [0, M], i = 1, \dots, L-1$. Now, by substituting S_{L-1}^* in (4), it is sufficient to check S_L at $n_L = 0$ and $n_L = M$. By setting $n_L = 0$ in (4), we have $S_L = S_{L-1}$, and since $S_L^* > S_{L-1}^*$ and $S_{L-1}^* \geq S_{L-1}$, it can be inferred that $S_L^* > S_L$ for $n_i \in [0, M], i = 1, \dots, L-1$ and $n_L = 0$. In the case that $n_L = M$ in (4), we check whether the inequality in (31) is satisfied.

$$S_L^* > S_{L-1} \left(1 - \frac{1}{M}\right)^M + M \left(1 - \frac{1}{M}\right)^{M-1} \quad (31)$$

using the assumption $S_{L-1}^* > S_{L-1}$, we can check the following inequality instead of (31).

$$S_L^* > S_{L-1}^* \left(1 - \frac{1}{M}\right)^M + M \left(1 - \frac{1}{M}\right)^{M-1} \quad (32)$$

According to (4), S_{L-1}^* in (32) can be replaced by $S_L^* \left(1 - \frac{1}{M}\right)^{-n_L^*} - n_L^* \left(1 - \frac{1}{M}\right)^{-1}$, which results in (33).

$$S_L^* \left(1 - \left(1 - \frac{1}{M}\right)^{M-n_L^*}\right) > (M - n_L^*) \left(1 - \frac{1}{M}\right)^{M-1} \quad (33)$$

Now, by substituting the maximum value of S_L at n_L^* and ρ_L^* from (5) in (33), we have:

$$\left(1 - \frac{1}{M}\right)^{M-n_L^*} \left(1 + \ln\left(\frac{M}{M-1}\right)(M - n_L^*)\right) < 1 \quad (34)$$

where n_L^* is a value between 0 and M , according to what has been obtained in (7). The first-order derivative of the left term in (34) with respect to n_L^* is:

$$\left(\ln\left(\frac{M}{M-1}\right)\right)^2 (M - n_L^*) \left(1 - \frac{1}{M}\right)^{M-n_L^*} > 0$$

which is a positive value for all possible values of n_L^* . Thus, the left term in (34) is an increasing function of n_L^* and its maximum value, 1, happens at $n_L^* = M$. Then, the inequality in (34) is true for $n_L^* \in (0, M)$.

According to what has been discussed in this lemma, the value of S_L at the boundary of $\mathbf{dom} S_L$ is less than S_L^* and hence, $n_i^*, i = 1, \dots, L$ is the only global optimal point of the function S_L .

REFERENCES

1. Vermesan O, Friess P. Internet Of Things-From Research and Innovation to Market Deployment. Aalborg, Denmark: River Publisher, 1st edn. 2014.
2. Ghavimi F, Chen H-H. M2M Communications in 3GPP LTE/LTE-A Networks: Architectures, Service Requirements, Challenges, and Applications 2014. *IEEE Communications Surveys & Tutorials*; 17(2): 525-549.
3. 3GPP TS 36.321 V12.5.0. *Evolved Universal Terrestrial Radio Access (E-UTRA) Medium Access Control (MAC) protocol specification, Release 12*, 2015.
4. 3GPP TS 22.011 V12.1.0. *Technical Specification Group Services and System Aspects; Service accessibility, Release 12*, 2014; Available from: www.3gpp.org.
5. Thomsen H, Pratas NK, Stefanovic C, Popovski P. Code-expanded radio access protocol for machine-to-machine communications 2013. *Transaction on Emerging Telecommunications Technologies*; 24(4): 355-365.
6. Kim JS, Munir D, Hasan SF, Chung MY. Enhancement of LTE RACH through extended random access process 2014. *Electronics Letters*; 50(19): 1399-1400.
7. 3GPP TR 37.868 V11.0.0. *Study on RAN Improvements for Machine-Type Communications*, 2011.
8. Yang Y, Yum TP. Analysis of power ramping schemes for UTRA-FDD random access channel 2005. *IEEE Transaction of Wireless Communications*; 4(6): 2688-2693.
9. Arouk O, Ksentini A, Taleb T. Group Paging-based Energy Saving for Massive MTC Accesses in LTE and Beyond Networks 2016. *IEEE Journal on Selected Area in Communications*; 34(5): 1086-1102.
10. Ferdouse L, Anpalagan A, Misra S. Congestion and overload control techniques in massive M2M systems: a survey 2015. *Transactions on Emerging Telecommunications Technologies*; DOI: 10.1002/ett.2936.

11. Wu H, Zhu C, La R, Liu X, Zhang Y. FASA: Accelerated S-ALOHA Using Access History for Event-Driven M2M Communications 2013. *IEEE/ACM Transactions on Networking*; 21(6): 1904-1917.
12. Arouk O, Ksentini A. Multi-Channel Slotted Aloha Optimization for Machine-Type-Communication. in *Proceedings of the 17th ACM International Conference on Modeling, Analysis and Simulation of Wireless and Mobile Systems, ser. MSWiM 14*, 2014; 119-125.
13. Ksentini A, Hadjadj-Aoul Y, Taleb T. Cellular-Based Machine-to-Machine: Overload Control 2012. *IEEE Network*; 26(6): 54-60.
14. Alavikia Z, Ghasemi A. Overload control in the network domain of LTE/LTE-A based machine type communications 2016. *Wireless Networks*; DOI:10.1007/s11276-016-1310-3.
15. Cheng RG, Chen J, Chen DW, Wei CH. Modeling and Analysis of an Extended Access Barring Algorithm for Machine-type Communications in LTE-A Networks 2015. *IEEE Transactions on Wireless Communications*; 14(6): 2956-2968.
16. Yang X, Fapojuwo A, Egbogah E. Performance Analysis and Parameter Optimization of Random Access Backoff Algorithm in LTE. *IEEE Vehicular Technology Conference (VTC 2012)*, 2012; 1-5.
17. 3GPP TSG, RAN WG2 Meeting 71 R2-104662. *MTC simulation results with specific solutions, ZTE, Madrid, Spain, 23rd*, 2010.
18. Kim T, Seok-ko K, Bang I, Sung DK. A Random Access Scheme Based on a Special Preamble for Supporting Emergency Alarms. *IEEE Wireless Communications and Networking Conference (WCNC 2014)*, 2014; 1768-1773.
19. Yue W. The effect of capture on performance of multichannel slotted ALOHA systems 1991. *IEEE Transactions on Communications*; 39(6): 818-822.
20. Sarker JH. Stable and unstable operating regions of slotted ALOHA with number of retransmission attempts and number of power levels 2006. *IEE Proceedings - Communications*; 153(3): 355-364.
21. Khoshnevis B, Khalaj BH. Analysis of a deterministic power level selection algorithm with small and large power steps for Aloha networks under saturation 2007. *Wireless Networks*; 15(3): 407-418.
22. Khoshnevis B, Khalaj BH. Optimum power selection algorithms in Aloha networks: random and deterministic approaches 2007. *IEEE transactions on wireless communications*; 6(8): 3124-3136.
23. Choi YJ, G-Shin K. Joint collision resolution and transmit-power adjustment for Aloha-type random access 2013. *Wireless Communications and Mobile Computing*; 13(2): 184-197.
24. Zou M, Chan S, Vu HL, Ping L. Throughput Improvement of 802.11 Networks via Randomization of Transmission Power Levels 2016. *IEEE Transactions on Vehicular Technology*; 65(4): 2703-2714.
25. 3GPP TS 36.211 V11.1.0. *Evolved Universal Terrestrial Radio Access (E-UTRAN); Physical channels and modulation, Release 11*, 2013.
26. Koseoglu M, Hwang D. Lower bounds on the LTE-A average random access delay under massive M2M arrivals 2016. *IEEE Transactions on Communications*; 64(5): 2104-2115.
27. Oh C-Y, Hwang D, Lee T-J. Joint access control and resource allocation for concurrent and massive access of M2M devices 2015. *IEEE Transactions on Wireless Communications*; 14(8): 4182-4192.
28. Zhang N, Kang G, Wang J, Guo Y, Labeau F. Resource Allocation in a New Random Access for M2M Communications 2015. *IEEE Communications Letters*; 19(5): 843-846.
29. T-Wiriatmadja D, Choi KW. Hybrid Random Access and Data Transmission Protocol for Machine-to-Machine Communications in Cellular Networks 2015. *IEEE Transactions on Wireless Communications*; 14(1): 33-46.
30. 3GPP TS 36.101 V12.7.0. *Evolved Universal Terrestrial Radio Access (E-UTRA); User Equipment (UE) radio transmission and reception, Release 12*, 2015.
31. Madueo GC, Nielsen JJ, Kim DM, Pratas NK, Stefanovic C, Popovski P. Assessment of LTE Wireless Access for Monitoring of Energy Distribution in the Smart Grid 2016. *IEEE Journal on Selected Areas in Communications*; 34(3): 675-688.
32. 3GPP TS 36.213 V12.4.0. *Evolved Universal Terrestrial Radio Access (E-UTRA); Physical layer procedures, Release 12*, 2015.
33. Abramowitz M, Stegun IA. *Handbook of Mathematical Functions with Formulas, Graphs, and Mathematical Tables*. New York: Dover, 1965.
34. Fitzpatrick PM. *Advanced Calculus. Volume 5*, Maryland, Boston: American Mathematical Society: PWS Publishing, 2st, 2006.